IOPscience

Hadron mass corrections in semi-inclusive deep inelastic scattering

JHEP11(2009)084

Hadron mass corrections in semi-inclusive deep inelastic scattering

A. Accardi,[a,b] **T. Hobbs**[b] **and W. Melnitchouk**[b]

[a] *Hampton University,*
Hampton, Virginia 23668, U.S.A.

[b] *Jefferson Lab,*
Newport News, Virginia 23606, U.S.A.

E-mail: accardi@jlab.org, thobbs@jlab.org, wmelnitc@jlab.org

ABSTRACT: We derive mass corrections for semi-inclusive deep inelastic scattering of leptons from nucleons using a collinear factorization framework which incorporates the initial state mass of the target nucleon and the final state mass of the produced hadron. The formalism is constructed specifically to ensure that physical kinematic thresholds for the semi-inclusive process are explicitly respected. A systematic study of the kinematic dependencies of the mass corrections to semi-inclusive cross sections reveals that these are even larger than for inclusive structure functions, especially at very small and very large hadron momentum fractions. The hadron mass corrections compete with the experimental uncertainties at kinematics typical of current facilities, and will be important to efforts at extracting parton distributions or fragmentation functions from semi-inclusive processes at intermediate energies.

Contents

1 Introduction

In recent years semi-inclusive deep inelastic scattering (SIDIS) has received much attention as a tool to investigate various aspects of hadron structure, such as the flavor dependence of the nucleon's parton distribution functions, both unpolarized and polarized, through flavor tagging of hadrons in the final state. Observation of the momentum distribution of produced hadrons also allows access to the largely unexplored transverse momentum dependent parton distributions, which reveal a much richer landscape of the spin and momentum distribution of quarks in the nucleon, and which are the subject of increasingly greater focus at modern facilities such as Jefferson Lab.

At high energies the scattering and hadronization components of the SIDIS process factorize and the cross section can be represented as a product of parton distribution and fragmentation functions. In practice, however, experiments are often carried out at few-GeV energies with Q^2 as low as $1\,\mathrm{GeV}^2$, suggesting that $1/Q^2$ power corrections must be controlled in order to determine the applicability of partonic analyses of the data.

One of the standard finite-Q^2 corrections that must be applied in analyses of *inclusive* deep inelastic scattering (DIS) data is target mass corrections (TMCs) [1]. Kinematical in origin, TMCs arise from leading twist operators in QCD, but enter as $1/Q^2$ corrections to structure functions [2]. They are especially egregious at high values of the Bjorken scaling variable x_B, even at relatively large Q^2, and are crucial for reliable extractions of parton distributions in this region. To date, however, the phenomenology of TMCs has not been systematically considered in SIDIS, and we do so in this paper.

Target mass corrections in inclusive DIS have usually been formulated within the operator product expansion, in which the subleading $1/Q^2$ corrections arise from twist-two

operators involving derivative insertions into quark bilinears [3–9]. Unfortunately, this method cannot be rigorously extended to the production of hadrons in the final state. An alternative approach to computing TMCs makes use of the collinear factorization (CF) framework [10–12], which has recently been used in both unpolarized [13–15] and polarized [16] inclusive DIS. Because here one works directly in momentum space, the method can be readily extended to SIDIS. In contrast to inclusive DIS, where the only mass scale entering the problem is that of the target hadron, in SIDIS finite-Q^2 corrections arise from both the target mass and the mass of the produced hadron. For generality we shall refer to their combined effects as "hadron mass corrections" (HMCs).

Hadron mass corrections in SIDIS at finite-Q^2 kinematics in CF were considered previously in refs. [17, 18] in different collinear frames. Albino et al. [17] studied the effects of the final state hadron mass, but did not consider the effects of the target mass. Mulders [18] derived corrections due to both target and produced hadron mass, but did not discuss the phenomenological consequences. Neither of these, however, addressed problems related to kinematic thresholds.

In this work we use the CF framework to derive the mass corrections to the SIDIS cross section at finite Q^2, and systematically investigate their implications at kinematics relevant to current experiments. The formalism is constructed specifically to ensure that physical kinematic thresholds for the semi-inclusive process are explicitly respected. In section 2 we review the collinear formalism and discuss its application to semi-inclusive hadron production. To expose the origin of the corrections we work at leading order in α_s; next-to-leading order effects can be included in subsequent analyses. In section 3 we explore the relative importance of the HMCs numerically, and evaluate the size of the corrections in the cross sections and fragmentation functions at various kinematics. To assess their possible impact on data analyses, we also compare the magnitude of the HMCs at kinematics typical of modern facilities, such as Jefferson Lab and HERMES, with experimental errors from recent experiments. Finally, in section 4 we summarize our results and outline avenues for future developments of this work. A discussion of the formulation of HMCs in different collinear frames is presented in appendix A.

2   Semi-inclusive scattering at finite Q^2

We begin the discussion of SIDIS at finite values of the photon virtuality Q^2 by defining the relevant kinematics and momentum variables in a collinear frame, and introduce the hadronic tensor computed in a covariant parton model. Collinear factorization is then performed in the leading order approximation in which the produced hadron is effectively collinear with the scattered parton, which more directly reveals the effects of hadron masses on the cross sections and fragmentation functions.

2.1 External kinematics

The four-momenta of the target nucleon (p), virtual photon (q) and produced hadron h (p_h) can be decomposed in terms of light-cone unit vectors n and $\overline{n}$ as [10]

$$p^\mu = p^+ \overline{n}^\mu + \frac{M^2}{2p^+} n^\mu \,, \tag{2.1a}$$

$$q^\mu = -\xi p^+ \overline{n}^\mu + \frac{Q^2}{2\xi p^+} n^\mu \,, \tag{2.1b}$$

$$p_h^\mu = \frac{\xi m_{h\perp}^2}{\zeta_h Q^2} p^+ \overline{n}^\mu + \frac{\zeta_h Q^2}{2\xi p^+} n^\mu + p_{h\perp}^\mu \,, \tag{2.1c}$$

where M is the target nucleon mass, $Q^2 = -q^2$, and the light-cone vectors satisfy $n^2 = \overline{n}^2 = 0$ and $n \cdot \overline{n} = 1$. Here we define light-cone components of any four-vector v by $v^+ = v \cdot \overline{n} = (v_0 + v_z)/\sqrt{2}$ and $v^- = v \cdot n = (v_0 - v_z)/\sqrt{2}$. The momenta p and q are chosen to lie in the same plane as n and $\overline{n}$, as for inclusive DIS. We call this the (p,q) collinear frame; other possible choices are discussed and compared in appendix A. The nucleon plus-momentum p^+ can be interpreted as a parameter for boosts along the z-axis, connecting the target rest frame to the infinite-momentum frame; the target rest frame $(p^+ = M/\sqrt{2})$ and the Breit frame $(p^+ = Q/(\sqrt{2}\xi))$ are part of this family of frames. The transverse momentum four-vector of the produced hadron $p_{h\perp}^\mu$ satisfies $p_{h\perp} \cdot n = p_{h\perp} \cdot \overline{n} = 0$, and we define the transverse mass squared as $m_{h\perp}^2 = m_h^2 - p_{h\perp}^2$, where m_h is the produced hadron mass, and the transverse four-vector squared is $p_{h\perp}^2 = -\boldsymbol{p}_{h\perp}^2$.

In the chosen collinear frame the variable $\xi = -q^+/p^+$ defined in eq. (2.1b) coincides with the finite-Q^2 Nachtmann scaling variable [2, 19],

$$\xi = \frac{2x_B}{1 + \sqrt{1 + 4x_B^2 M^2/Q^2}} \,, \tag{2.2}$$

which in the Bjorken limit $(Q^2 \to \infty$ at fixed $x_B)$ reduces to the Bjorken scaling variable $x_B = Q^2/2p \cdot q$. The scaling fragmentation variable $\zeta_h = p_h^-/q^-$ defined in eq. (2.1c) is related to the fragmentation invariant $z_h = p_h \cdot p/q \cdot p$ by

$$\zeta_h = \frac{z_h}{2} \frac{\xi}{x_B} \left(1 + \sqrt{1 - \frac{4x_B^2 M^2 m_{h\perp}^2}{z_h^2 \, Q^4}} \right) \,, \tag{2.3a}$$

and the positivity of the argument in the radical in eq. (2.3a) is ensured by the condition $E_h \geq m_{h\perp}$, which imposes

$$z_h \geq z_h^{\min} = 2x_B \frac{M m_h}{Q^2} \,. \tag{2.3b}$$

One can also define ζ_h in terms of the invariant $\eta_h = 2p_h \cdot q/q^2$ by

$$\zeta_h = \frac{\eta_h}{2} \left(1 + \sqrt{1 + \frac{4m_{h\perp}^2}{\eta_h^2 \, Q^2}} \right) \,, \tag{2.3c}$$
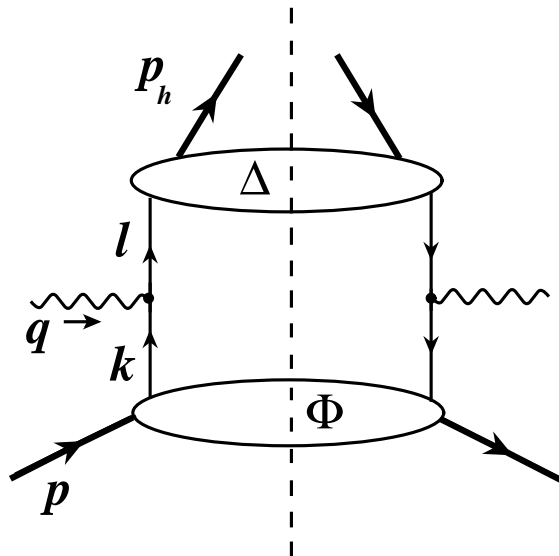
Figure 1. Kinematics of semi-inclusive deep inelastic lepton-nucleon scattering at leading order, producing a final state hadron h. The momenta of the target nucleon (p), virtual photon (q), incident (k) and scattered quarks (l), and the produced hadron (p_h) are labeled explicitly, with Φ and Δ denoting the correlators relevant to the quark distribution and fragmentation functions. The vertical dashed line represents the cut of the forward amplitude.

which is convenient for discriminating between the target and current fragmentation hemispheres in hadron production. Note that in the target rest frame $z_h = E_h/\nu$ is the usual ratio of the produced hadron to virtual photon energies. In the Breit frame $\eta_h = p_{hz}/q_z$ is the ratio of the longitudinal components of the hadron and photon energies, which can be used to define the current ($\eta_h > 0$) and target ($\eta_h < 0$) hemispheres for hadron production. In the Bjorken limit one has $\zeta_h \to z_h \to \eta_h$.

Conservation of four-momentum and baryon number impose an upper limit on the x_B variable,

$$x_B \leq \left(1 + \frac{m_h^2 + 2Mm_h}{Q^2}\right)^{-1} \equiv x_B^{\max},\qquad(2.4)$$

which corresponds to the exclusive production of a nucleon and a hadron h in the final state. Similarly the limits on the fragmentation variable ζ_h are given by

$$\frac{\xi}{1-\xi}\frac{M^2}{Q^2} \leq \zeta_h \leq 1 + \xi\frac{M^2}{Q^2},\qquad(2.5)$$

where the lower limit corresponds to diffractive production of the hadron h, and the upper limit reflects the fragmentation threshold, which approaches unity in the Bjorken limit.

2.2 Parton kinematics in collinear factorization

At the partonic level the SIDIS process at leading order in the strong coupling constant α_s is illustrated in figure 1. It proceeds through the scattering from a quark carrying a

light-cone momentum fraction $x = k^+/p^+$, which then fragments to a hadron h carrying a light-cone momentum fraction $z = p_h^-/l^-$, where k and l are the four-momenta of the initial and scattered quarks. At higher orders the hard scattering can also take place from a gluon, and additional partons can be created in the collision.

The parton momenta k and l can be parametrized in terms of the light-cone vectors n and $\bar{n}$ as

$$k^\mu = xp^+ \bar{n}^\mu + \frac{k^2 + k_\perp^2}{2xp^+} n^\mu + k_\perp^\mu \,, \tag{2.6a}$$

$$l^\mu = \frac{l^2 + l_\perp^2}{2p_h^-/z} \bar{n}^\mu + \frac{p_h^-}{z} n^\mu + l_\perp^\mu \,, \tag{2.6b}$$

with the parton transverse momentum four-vectors $k_\perp$ and $l_\perp$ orthogonal to n and $\bar{n}$. In collinear factorization the hard scattering amplitude is expanded around on-shell and collinear momenta $\tilde{k}$ and $\tilde{l}$,

$$\tilde{k}^\mu = xp^+ \bar{n}^\mu + \frac{\tilde{k}^2}{2xp^+} n^\mu \tag{2.7a}$$

$$\tilde{l}^\mu = \frac{\tilde{l}^2 + p_{h\perp}^2/z^2}{2p_h^-/z} \bar{n}^\mu + \frac{p_h^-}{z} n^\mu + \frac{p_{h\perp}^\mu}{z} \,, \tag{2.7b}$$

where the initial and final collinear parton "masses" $\tilde{k}^2$ and $\tilde{l}^2$ are kept for generality.

Defining the invariant $\hat{x} = -q^2/2\tilde{k} \cdot q$ as the partonic analog of the Bjorken variable x_B, at finite Q^2 one has

$$\hat{x} = \frac{\xi}{x} \left(1 + \frac{x}{\xi} \frac{\tilde{k}^2}{Q^2}\right) \,. \tag{2.8}$$

Using the methods described in ref. [15] one can show that for SIDIS cross sections integrated over $p_{h\perp}$, $\hat{x}$ is constrained to be in the range

$$1 + \frac{m_h^2}{\zeta_h Q^2} - \frac{\tilde{k}^2}{Q^2} \left(1 - \frac{\xi m_h^2}{x\zeta_h Q^2}\right) \leq \frac{1}{\hat{x}} \leq \frac{1}{x_B} \left(1 - x_B \frac{2Mm_h + \tilde{k}^2}{Q^2}\right) \,, \tag{2.9}$$

where the lower limit arises from the minimum of the current jet mass, and the upper limit corresponds to collinear spectators with minimal mass. These limits agree with the limit on x_B in eq. (2.4) for any $\tilde{k}^2 \geq x(\zeta_h - 1)Q^2/\xi$. For the fragmentation process one finds analogous limits on ζ_h,

$$\zeta_h \leq \frac{1}{z} \zeta_h \leq 1 + \frac{\xi}{x} \frac{\tilde{k}^2}{Q^2} \,, \tag{2.10}$$

which agrees with the limit in eq. (2.5), provided that $\tilde{k}^2 \leq xM^2$. The requirement that the collinear parton masses be independent of the parton momentum (*viz.*, independent of x) implies $\tilde{k}^2 \leq 0$. Combined with the above lower limit on $\tilde{k}^2$, this naturally leads to a collinear expansion around a massless initial state parton, $\tilde{k}^2 = 0$.

The choice of $\tilde{l}^2$ is made by considering the cross section at leading order in α_s. Four-momentum conservation for the hard scattering, together with the choice $\tilde{k}^2 = 0$, leads to the relations $x = \xi(1 + \tilde{l}^2/Q^2) \equiv \xi_h$ and $z = \zeta_h$. Clearly z falls within the kinematic limits (2.10). However, in order for x to respect the limits (2.9) we choose $\tilde{l}^2 = m_h^2/\zeta_h$, in which case

$$\xi_h = \xi \left(1 + \frac{m_h^2}{\zeta_h Q^2}\right). \tag{2.11}$$

While larger values of $\tilde{l}^2$ would also allow x to fall within the limits (2.9), this choice is the closest to the physical quark mass.

We stress that our prescription for the collinear parton masses $\tilde{k}^2$ and $\tilde{l}^2$ is dictated by the external kinematic limits in eqs. (2.4) and (2.5), which are independent of the parton model and collinear factorization approximations. As discussed in refs. [15, 21], this is crucial when considering cross sections close to the kinematic limits, such as at large x_B or large z_h. However, as we shall see in the next section, the SIDIS cross section can also receive non-negligible corrections at small x_B since $\xi_h > \xi \approx x_B$. This is qualitatively different from the behavior of the target mass corrections in inclusive DIS, which are always suppressed at small x_B [15].

2.3   Hadron tensor and cross section at leading order

In collinear factorization the hadron tensor at leading order, to which we restrict the rest of our analysis, can be written as

$$2MW^{\mu\nu}(p, q, p_h) = \sum_q e_q^2 \int d^4k \; d^4l \; \delta^{(4)}(\tilde{k} + q - \tilde{l}) \; \text{Tr}[\Phi_q(p, k) \gamma^\mu \Delta_q^h(l, p_h) \gamma^\nu], \tag{2.12}$$

where the sum is taken over quark flavors q, and the correlators Φ_q and Δ_q^h encode the relevant quark distribution and fragmentation functions, respectively [11, 12, 18]. According to our prescription for the collinear momenta, the δ-function depends on the collinear momenta $\tilde{k}$ and $\tilde{l}$, so that integrations over $dk^- \, d^2k_\perp$ and $dl^+ \, d^2l_\perp$ act directly on the correlators Φ and Δ. The leading twist part of the cross section can then be extracted by retaining the $\bar{\slashed{n}}$ and $\slashed{n}$ components in the Dirac structure expansion of the integrated correlators,

$$\int dk^- d^2k_\perp \, \Phi_q(p, k) = \frac{1}{2} f_q(x) \bar{\slashed{n}} + \dots, \tag{2.13a}$$

$$\int dl^+ d^2l_\perp \, \Delta_q^h(l, p_h) = \frac{1}{2} D_q^h(z) \slashed{n} + \dots, \tag{2.13b}$$

where the dots indicate contributions of higher twist [20]. The nonperturbative quark distribution function $f_q(x)$ and quark-to-hadron fragmentation function $D_q^h(z)$ are explicitly

defined as

$$
\begin{aligned}
f_q(x) &= \frac{1}{2} \int dk^- d^2 k_\perp \, \mathrm{Tr} \left[\gamma^+ \Phi_q(p,k) \right]_{k^+=xp^+} \\
&\overset{\mathrm{LC}}{=} \frac{1}{2} \int \frac{dw^-}{2\pi} e^{ixp^+w^-} \langle N|\overline{\psi}_q(0)\, \gamma^+\, \psi_q(w^- n)|N\rangle \,,
\end{aligned}
\tag{2.14a}
$$

$$
\begin{aligned}
D_q^h(z) &= \frac{z}{2} \int dl^+ d^2 l_\perp \, \mathrm{Tr} \left[\gamma^- \Delta_q^h(l,p_h) \right]_{l^-=p_h^-/z} \\
&\overset{\mathrm{LC}}{=} \frac{z}{2} \sum_X \int \frac{dw^+}{2\pi} e^{i(p_h^-/z)w^+} \langle 0|\psi_q(w^+ n)|h,X\rangle\langle h,X|\overline{\psi}_q(0)\gamma^-|0\rangle \,,
\end{aligned}
\tag{2.14b}
$$

where "LC" denotes use of the light-cone gauge, and the fragmentation function is normalized such that $\sum_h \int_0^1 dz\, z\, D_q^h(z) = 1$ [18].

From eq. (2.12) the energy-momentum conserving δ-function can be decomposed along the plus, minus, and transverse components of the light-cone momentum. The plus and minus components yield a product of δ-functions that fix $x = \xi_h$ and $z = \zeta_h$, while the transverse component constrains the transverse momentum of the scattered quark to vanish, which restricts the produced hadrons to be purely longitudinal, $p_{h\perp} = z\, l_\perp = 0$. Hadrons with nonzero transverse momentum can be generated from higher order perturbative QCD processes, or from intrinsic transverse momentum in the parton distribution functions, as in the case of transverse momentum dependent distributions [20], but are not considered in this work. The resulting hadron tensor in the presence of hadron mass effects,

$$
2MW^{\mu\nu}(p,q,p_h) = \frac{\zeta_h}{4} \sum_q e_q^2 \, \delta^{(2)}(\boldsymbol{p}_\perp)\mathrm{Tr}\left[\slashed{\overline{n}}\gamma^\mu\slashed{n}\gamma^\nu\right] f_q(\xi_h)D_q^h(\zeta_h) \,,
\tag{2.15}
$$

is then factorized into a product of parton distribution and fragmentation functions evaluated at the finite-Q^2 scaling variables ξ_h and ζ_h, instead of x_B and z_h as would be obtained in the massless case, and recovered from eq. (2.15) in the Bjorken limit. Note that this prescription is the same as that used in ref. [15] when discussing inclusive DIS in the presence of jet mass corrections, and is close in spirit to that advocated in ref. [21], where the trace is calculated as in the massless case, but overall parton momentum conservation respects the external kinematics.

Finally, the SIDIS cross section is computed by contracting the hadron tensor with an analogous lepton tensor [20], leading to

$$
\sigma \equiv \frac{d\sigma}{dx_B\, dQ^2\, dz_h} = \frac{2\pi\alpha_s^2}{Q^4} \frac{y^2}{1-\varepsilon} \frac{d\zeta_h}{dz_h} \sum_q e_q^2 \, f_q(\xi_h, Q^2)\, D_q^h(\zeta_h, Q^2) \,,
\tag{2.16}
$$

where the dependence of the functions on the scale Q^2 is made explicit, and the Jacobian $d\zeta_h/dz_h = (1 - M^2\xi^2/Q^2)/(1 - \xi^2 M^2 m_h^2/\zeta_h^2 Q^4)$. In eq. (2.16) the variable y defined as $y = p \cdot q/p \cdot p_\ell$, where p_ℓ is the lepton momentum, represents the fractional energy transfer from the lepton to the hadron in the target rest frame ($y = \nu/E$, with E the lepton energy), and $\varepsilon = (1 - y - y^2\gamma^2/4)/(1 - y + y^2[1/2 + \gamma^2/4])$ is the ratio of longitudinal to transverse photon flux, with $\gamma^2 = 4x_B^2 M^2/Q^2$. The cross section differential in η_h can be obtained
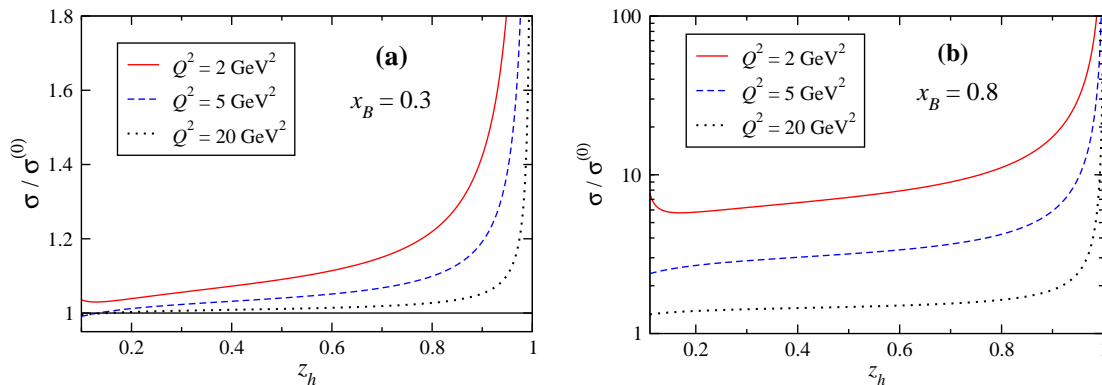
Figure 2. Ratio of cross sections $\sigma/\sigma^{(0)}$ for semi-inclusive charged-pion production $((\pi^+ + \pi^-)/2)$ as a function of z_h at several Q^2 values for (a) $x_B = 0.3$ and (b) $x_B = 0.8$.

using $d\zeta_h/d\eta_h = 1/(1+m_h^2/\zeta_h^2 Q^2)$ instead of $d\zeta_h/dz_h$. It is interesting to observe that since ξ_h depends explicitly on m_h and ζ_h depends on z_h and x_B, at finite Q^2 the scattering and fragmentation parts of the cross section (2.16) are not independent.

As a final remark we note that at the maximum allowed x_B for SIDIS, eq. (2.4), the value of ξ_h is smaller than $\xi_h(x_B = x_B^{\max}) < 1$. As in the case of inclusive DIS [15], the SIDIS cross section therefore does not vanish as $x_B \to x_B^{\max}$, which is a manifestation of the well-known threshold problem [1]. On the other hand, from eq. (2.10) the fragmentation variable $\zeta_h \leq 1$, and no threshold problem appears in the fragmentation function since $D(\zeta_h) \to 0$ as $\zeta_h \to 1$.

In the next section we shall examine the phenomenological consequences of the finite-Q^2 rescaling of the SIDIS cross section numerically.

3 Hadron mass corrections

Using the hadron mass corrected expressions for the SIDIS cross section derived above, we next explore the dependence of the cross sections and fragmentation functions on the fragmentation variable z_h, for various x_B and Q^2 values and for different final state hadron masses. We then compare the relative size of the HMCs with the experimental uncertainties from recent SIDIS experiments at Jefferson Lab and the HERMES Collaboration, as well as with higher energy data from the European Muon Collaboration (EMC) and HERA.

3.1 HMC phenomenology

To illustrate most directly the effects of the HMCs, in figure 2 we consider charged pion production (average of π^+ and π^-) and plot as a function of z_h, for different x_B and Q^2, the ratio of the full cross section σ in eq. (2.16) to the cross section $\sigma^{(0)}$, defined by taking the massless limit for the scaling variables $\sigma^{(0)} \equiv \sigma(\xi_h \to x_B, \zeta_h \to z_h)$ and setting $d\zeta_h/dz_h = 1$. For the numerical computations we use the leading order CTEQ6L parton distributions [22] and the KKP leading order fragmentation functions [23], unless otherwise specified. The ratio at $x_B = 0.3$ in figure 2(a) is enhanced by $\leq 20\%$ at $Q^2 = 2\,\text{GeV}^2$ for
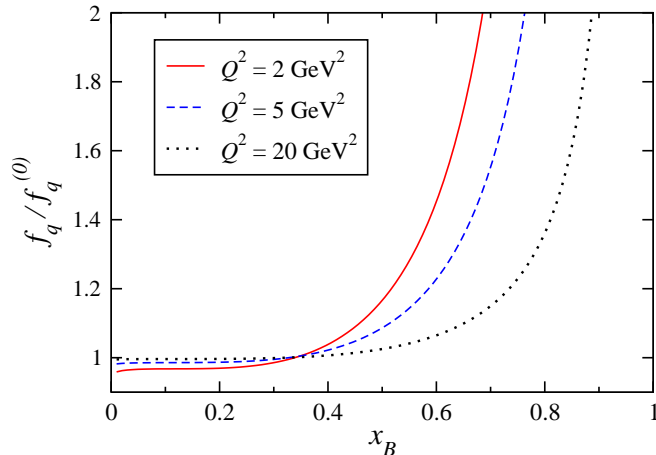
Figure 3. Ratio of the hadron mass corrected isoscalar parton distribution function $f_q(\xi_h)$ for $q = u + d$ to the massless limit distribution $f_q^{(0)}$ as a function of x_B, for $m_h = m_\pi$ and $\zeta_h = 0.2$.

$z_h \lesssim 0.7$, but rises dramatically as $z_h \to 1$. The effect is naturally smaller at higher Q^2 values, but the rise at high z_h is a common feature for all kinematics. The same ratios at $x_B = 0.8$ in figure 2(b) show approximately an order of magnitude larger overall effect (note the logarithmic scale!).

The small upturn in the ratios at low z_h for the lowest Q^2 in figure 2 can be understood from the interplay between the finite-Q^2 kinematics and the shape of the fragmentation function. Assuming the fragmentation function is smooth, one can expand the ratio of corrected to uncorrected functions in a Taylor series as

$$\frac{D(\zeta_h)}{D(z_h)} \approx 1 + \frac{D'(z_h)}{D(z_h)}(\zeta_h - z_h)\,. \tag{3.1}$$

The z_h dependence of the HMCs arising in the fragmentation function is mostly determined by the negative shift in the fragmentation variable $(\zeta_h - z_h)$ and by the local rate of change over z_h of the fragmentation function. The pion fragmentation function generally behaves as a negative power of z_h at small z_h, and the negative slope drives the ratio of corrected to uncorrected fragmentation functions upward as $z_h \to z_h^{\min}$, where $|\zeta_h - z_h|$ is maximum. For kaons and protons the slope of the form factor can be positive, which would suppress the mass corrected cross section in the vicinity of $z_h^{\min}$. In the limit $z_h \to 1$, on the other hand, the ratio $\sigma/\sigma^{(0)}$ becomes divergent for any kinematics and any hadron species because the cross section $\sigma^{(0)} \propto D(z_h)$ vanishes, while the rescaled cross section remains finite.

At very small values of z_h the factor $(1 + m_h^2/\zeta_h Q^2)$ in the definition of ξ_h in eq. (2.11) can render ξ_h larger than x_B, suppressing the ξ_h-rescaled parton distributions relative to their asymptotic limit and driving $\sigma/\sigma^{(0)}$ slightly below unity. As discussed below, for heavier hadrons this effect will be more pronounced. The effect of the ξ_h rescaling on the SIDIS cross section is illustrated explicitly in figure 3, where we show the ratio of the isoscalar parton distribution functions f_q, $q = u + d$, with $[f_q = f_q(\xi_h)]$ and without $[f_q^{(0)} = f_q(x_B)]$ hadron mass corrections, as a function of x_B for $\zeta_h = 0.2$ and $m_h = m_\pi$. At $Q^2 = 2\,\text{GeV}^2$ the mass corrected parton distribution is several times larger than the
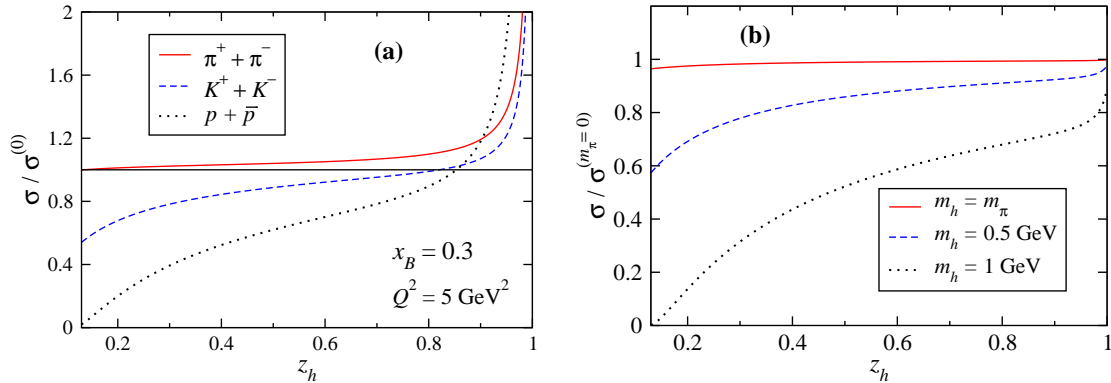
Figure 4. (a) Dependence of the ratio of SIDIS cross sections $\sigma/\sigma^{(0)}$ with and without HMCs for different produced hadrons, $h = \pi^+ + \pi^-$, $K^+ + K^-$ or $p + \bar{p}$. (b) Ratio of cross sections for $h = \pi^+ + \pi^-$ for different values of the pion mass, relative to the massless cross section. In both cases the kinematics chosen are $x_B = 0.3$ and $Q^2 = 5$ GeV^2.

uncorrected one at $x_B = 0.8$, and even at $Q^2 = 20\,\text{GeV}^2$ the HMC is some 50%, with the effect increasing dramatically as $x_B \to 1$. This sharp rise is analogous to that in inclusive DIS [15], and arises from ξ_h being smaller than x_B when the latter is large. This is responsible for the large overall magnitude of the corrections in figure 2(b) compared with those at $x_B = 0.3$. In contrast, the ξ_h rescaling effect becomes quite small at $x_B \lesssim 0.3$ for all the Q^2 considered, and in fact drives the ratio below unity, as discussed above.

The relative importance of HMCs for different produced hadron species is illustrated in figure 4(a), where the ratio $\sigma/\sigma^{(0)}$ is shown as a function of z_h for $x_B = 0.3$ and $Q^2 = 5$ GeV^2. Over the range $0.3 \lesssim z_h \lesssim 0.8$ the HMCs yield an upward correction of $\lesssim 10\%$ for the pions, but a downward correction of $\lesssim 20\%$ and $\lesssim 40\%$ for kaons and protons/antiprotons, respectively. At lower z_h the cross section ratio for the heavier hadrons decreases dramatically because of the large suppression of the parton distribution from the $(1 + m_h^2/\zeta_h Q^2)$ factor in ξ_h, which overwhelms any other small-z_h effect.

Note that in figure 4(a) the appropriate fragmentation function for each produced hadron species has been used, which introduces a flavor dependence in the HMC because of the different fragmentation function shapes for each hadron. To isolate the effects of the hadron mass alone, in figure 4(b) the ratios of cross sections computed with charged pion fragmentation functions and masses $m_h = m_\pi$ ($= 0.139\,\text{GeV}$), $0.5\,\text{GeV}$ and $1\,\text{GeV}$ are shown relative to the cross section with $m_\pi = 0$, for which $\zeta_h = z_h \xi/x_B$. One can see that in general increasing the hadron mass suppresses the cross section because of the ξ_h scaling, and the reshuffling of the HMC hierarchy in figure 4(a) going from low to high z_h is due to the increasingly negative large-z slope of the fragmentation functions for kaons and protons. While the differences at the physical pion mass are very small, for larger hadron masses $\sim 1\,\text{GeV}$ the effects can be quite significant at $z_h \lesssim 0.4$ even for Q^2 values of several GeV^2.
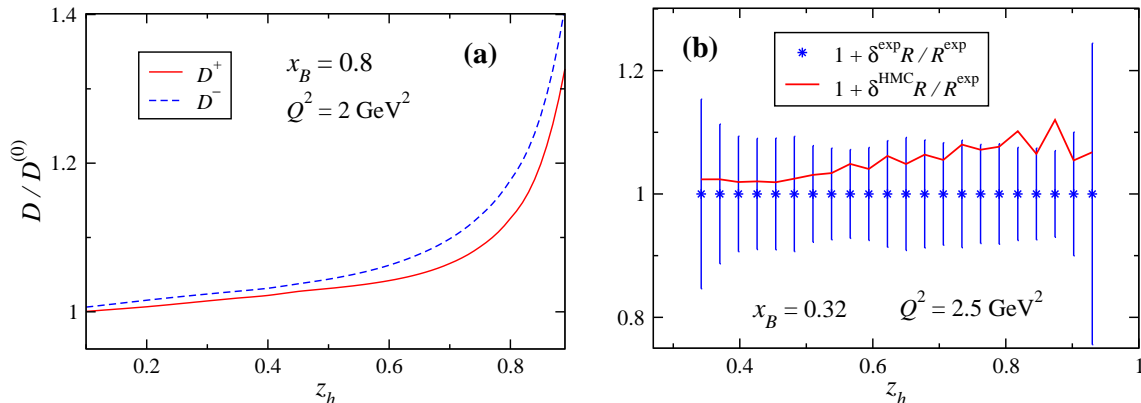
Figure 5. (a) Ratio of hadron mass corrected to uncorrected fragmentation functions $D/D^{(0)}$ for favored (solid) and unfavored (dotted) production of π^+, for $x_B = 0.8$ and $Q^2 = 2\,\mathrm{GeV}^2$. (b) Comparison of the hadron mass correction $\delta^{\mathrm{HMC}}R$ to the ratio of unfavored to favored fragmentation functions $R = D^-/D^+$ with experimental errors $\delta^{\mathrm{exp}}R$ on R from the recent Jefferson Lab experiment E00-108 [25], normalized to the central values of the data points.

3.2 Implications for experiments

One of the unique capabilities of SIDIS is the ability to tag individual quark flavors by selecting specific hadrons in the final state. For example, because of its valence quark content, production of π^+ is mostly sensitive to the u quark, requiring only a single $q\bar{q}$ pair creation from the vacuum, while π^- reflects mostly the d quark content of the target nucleon. This simple picture of primary fragmentation provides a good approximation to the production mechanism only at large z_h, however, and at low z_h secondary fragmentation involving two or more $q\bar{q}$ pair productions dilutes the direct flavor tagging. The primary fragmentation process is parametrized by the "favored" fragmentation function D^+, describing $u \to \pi^+$ or $d \to \pi^-$ hadronization, while the secondary fragmentation is parametrized by the "unfavored" fragmentation function D^-, describing $u \to \pi^-$ or $d \to \pi^+$ hadronization.

Because the D^+ and D^- functions have rather different z_h dependence, with unfavored fragmentation strongly suppressed at large z_h, they will be affected differently by the hadron mass corrections: one would expect larger HMCs for the unfavored process since the magnitude of the slope $|dD(z_h)/dz_h|$ in eq. (3.1) is larger for D^- than for D^+. In figure 5(a) one observes precisely this; here, we provide an upper limit (given the choice of $x_B = 0.8$ and $Q^2 = 2\,\mathrm{GeV}^2$) to the relative size of the mass effect in $D/D^{(0)}$, which is universally larger in the unfavored fragmentation function. In the numerical computations we have used the favored and unfavored fragmentation functions from ref. [24]. At lower x_B the correction will be smaller, although the qualitative features of the effect will remain.

The relevance of the HMCs to experimental data on the ratio $R = D^-/D^+$ is expressed in figure 5(b), which directly compares the difference $\delta^{\mathrm{HMC}}R = (D^-/D^+) - (D^-/D^+)^{(0)}$ to the statistical uncertainty $\delta^{\mathrm{exp}}R$ in the extracted values of R from the recent Jefferson Lab experiment E00-108 [25] at $x_B = 0.32$ and $Q^2 \approx 2.5\,\mathrm{GeV}^2$, with both quantities normalized to the central values of the measured R ratio. While at small z_h the HMC is relatively small compared with the experimental errors, at large z_h ($\gtrsim 0.6$) it begins to compete with the ex-
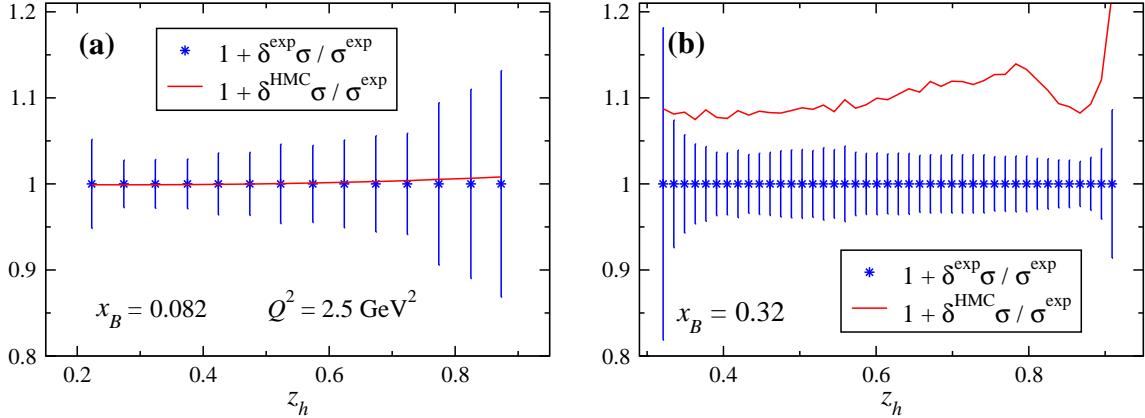
Figure 6. Comparison of the hadron mass correction to the SIDIS cross section for charged hadron production, $\delta^{\mathrm{HMC}}\sigma$, relative to the experimental cross section, $\delta^{\mathrm{exp}}\sigma$, with the relative experimental uncertainty as a function of z_h for (a) HERMES experiment [26] at $Q^2 = 2.5\,\mathrm{GeV}^2$ and $x_B = 0.082$, and (b) Jefferson Lab experiment E00-108 [25] at a similar Q^2 but at $x_B = 0.32$.

perimental uncertainty, suggesting that the hadron mass here poses a non-negligible effect.

The importance of the hadron mass corrections for experimental cross sections is examined in figure 6, where we compare the calculated difference $\delta^{\mathrm{HMC}}\sigma \equiv \sigma - \sigma^{(0)}$ with the experimental uncertainties $\delta^{\mathrm{exp}}\sigma$, normalized to the central values of the cross section for charged hadron production from HERMES [26] and Jefferson Lab [25]. Since both experiments are dominated by the semi-inclusive production of pions, so that $\xi_h \approx \xi$, HMCs generally produce upward shifts relative to data. The mass corrections at the HERMES kinematics in figure 6(a), where $Q^2 \approx 2.5\,\mathrm{GeV}^2$ and $x_B = 0.082$, are generally very small compared with the size of the experimental uncertainties. At higher energies, HMCs to fixed-angle measurements by the EMC [27] at large x_B values are also found to be negligible due to suppression by Q^2, which increases with x_B. Were these experiments conducted at smaller angles, however, it is likely that HMCs would become important.

On the other hand, for the Jefferson Lab experiment E00-108 [25] in figure 6(b) at a similar Q^2 but larger $x_B = 0.32$, the mass effects are approximately 2 times larger than the experimental statistical errors. This illustrates the potentially significant impact that HMCs can have on leading-twist analyses of SIDIS data at moderate and large x_B and low Q^2. To avoid these effects one would either need to go to smaller x_B or larger Q^2 values, for example afforded by the $12\,\mathrm{GeV}$ energy upgrade at Jefferson Lab. Alternatively, since the HMCs are calculated and model independent, lower Q^2 and higher x_B data will still yield useful leading twist information provided the mass corrections are accounted for.

Measurements at small $x_B \sim 0.001$ and $Q^2 \gtrsim 12\,\mathrm{GeV}^2$ have been performed by the H1 collaboration [31] at HERA, and the data presented in terms of the fragmentation invariant η_h. The phenomenology of HMCs is markedly different in terms of η_h from that discussed thus far in terms of z_h because of the different functional forms for ζ_h in eqs. (2.3), which constrains $\zeta_h > \eta_h$, and because of the Jacobian $d\zeta_h/d\eta_h$. In their analysis of the H1 data, Albino et al. [17] included the ζ_h rescaling of the fragmentation process, but

neglected the effects of the target mass, which would be problematic for heavier hadrons such as kaons and protons. The H1 Collaboration measured charged hadron multiplicities, dominated by pions ($\sim60\%$), with smaller contributions from kaons ($\sim30\%$) and protons ($\sim10\%$). In the measured Q^2 range the m_h^2/Q^2 term in ξ_h is therefore strongly suppressed and at the typically low x_B values one has $\xi \approx x_B$, so that overall we find the HMCs to be similar to those in ref. [17]. However, for identified kaons, and especially protons, the SIDIS cross section would be more strongly suppressed compared to the results of ref. [17] because $\xi_h \approx x_B(1+m_h^2/Q^2)$ is significantly larger than x_B. This suppression may be non-negligible for the extraction of kaon and proton fragmentation functions from small-x_B data.

4 Conclusions

In this paper we have derived hadron mass corrections to semi-inclusive deep inelastic cross sections at finite Q^2 and have performed a systematic exploration of their phenomenological consequences. Within the collinear factorization framework the modifications to the leading order SIDIS cross sections from initial and final state masses arise from a rescaling of the quark distribution and fragmentation functions in terms of the modified Nachtmann scaling variable ξ_h and a finite-Q^2 fragmentation variable ζ_h, respectively. The need for a modified Nachtmann variable is dictated by the requirement that the physical kinematic thresholds for the semi-inclusive process are explicitly respected.

We have examined the effects of the hadron mass corrections numerically at kinematics relevant to recent experiments, finding sizable effects at both small and large values of z_h, as well as for increasing x_B and m_h, and low Q^2. Our results emphasize the importance of controlling for such corrections in intermediate to high-x_B experiments executed at low Q^2, of which measurements at Jefferson Lab are typical, although not exclusive. We find that the hadron mass corrections can in some cases compete with the quoted experimental errors (as in the measurement of the ratio of unfavored to favored fragmentation functions D^-/D^+) or overwhelm them (as in the cross section measurements). Due to the presence of the modified Nachtmann variable the HMCs may also need to be considered for small-x_B collider experiments for the production of heavier hadrons such as kaons and protons, and their effects require further study.

The most direct use of the results presented here will be in leading twist analyses of SIDIS cross sections, where the HMCs must be included before extracting information on parton distribution and fragmentation functions, especially at large x_B and z_h. Application of this work can also be found in studies of semi-inclusive data in the nucleon resonance region, which has been the focus of attention recently in view of understanding the workings of quark-hadron duality [28–30].

While the present analysis has been performed at leading order in α_s, in the future we plan to extend the formalism to next-to-leading order, which will permit a more quantitative treatment of transverse mass dependence of the produced hadrons, $p_{h\perp} \neq 0$. It will also allow contact with transverse momentum dependent parton distributions, in which nonzero parton transverse momentum, $k_\perp \neq 0$, is an essential element. Finally, as in the inclusive DIS case, the SIDIS cross section corrected for hadron mass effects exhibits the threshold

problem which renders it nonzero as $x_B \to x_B^{\max}$. Solutions of this problem proposed in the literature for inclusive structure functions [4, 9, 15] will be extended to SIDIS in future work.

Acknowledgments

A Collinear frames in semi-inclusive DIS

A collinear frame in Minkowski space is defined by any two four-vectors. The intersection of the plane where they lie with the light-cone defines the light-cone four-vectors $\overline{n}^\mu$ and n^μ, that satisfy $n^2 = \overline{n}^2 = 0$ and $\overline{n} \cdot n = 1$. In SIDIS the hadronic tensor depends on the three vectors p^μ, q^μ and p_h^μ, which define three possible collinear frames denoted (p, q), (p_h, q) and (p_h, p). The (p, q) frame is the only frame that can be defined in DIS and is the one used in this work; the (p_h, q) frame is the only one that can be defined in semi-inclusive hadron production in e^+e^- collisions; and finally the (p_h, p) frame is typically preferred for analysis of transverse momentum dependent parton distributions in SIDIS.

In terms of the vectors p, q and p_h one can define two fragmentation invariants,

$$z_h = \frac{p_h \cdot p}{q \cdot p}, \qquad \eta_h = \frac{2p_h \cdot q}{q^2}, \tag{A.1}$$

which together with x_B, Q^2, M^2 and m_h^2 form a complete set of scalar Lorentz invariants in SIDIS. Because the variable η_h is defined independently of the target momentum, the effects of the final state hadron mass will decouple from those of the target mass in all reference frames. In contrast, z_h is defined in terms of both the target and produced hadron momenta, so that the target and hadron mass effects here will be entangled.

The light-cone fractional momentum ξ (Nachtmann variable) and the fragmentation variable ζ_h are defined in terms of the plus and minus components of the momenta as in eqs. (2.2) and (2.3a),

$$\xi = -\frac{q^+}{p^+}, \qquad \zeta_h = \frac{p_h^-}{q^-}. \tag{A.2}$$

We use these definitions in all three frames; however, in each frame the light-cone vectors (and therefore the plus and minus components of the four-momenta) will be different. In the following we discuss each of the three collinear frames and the consequences within each frame of the choice of fragmentation invariant.

(p, q) frame. In this frame the external vectors can be decomposed in terms of the light-cone vectors n and $\overline{n}$ as in eqs. (2.1),

$$p^\mu = p^+ \overline{n}^\mu + \frac{M^2}{2p^+} n^\mu \,, \tag{A.3a}$$

$$q^\mu = -\xi p^+ \overline{n}^\mu + \frac{Q^2}{2\xi p^+} n^\mu \,, \tag{A.3b}$$

$$p_h^\mu = \frac{m_{h\perp}^2}{\zeta_h Q^2/\xi} p^+ \overline{n}^\mu + \zeta_h \frac{Q^2}{2\xi p^+} n^\mu + p_{h\perp}^\mu \,, \tag{A.3c}$$

where $m_{h\perp}^2 = m_h^2 - p_{h\perp}^2 = m_h^2 + \boldsymbol{p}_{h\perp}^2$ is the transverse mass of the produced hadron. Inverting the definition of x_B, the Nachtmann scaling variable can be written as in eq. (2.2),

$$\xi = \frac{2x_B}{1 + \sqrt{1 + 4x_B^2 M^2/Q^2}} \,. \tag{A.4}$$

Similarly, the hadron fractional momentum ζ_h can be expressed in terms of either the fragmentation invariant z_h,

$$\zeta_h = \frac{z_h}{2} \frac{\xi}{x_B} \left(1 + \sqrt{1 - 4\frac{x_B^2}{z_h^2} \frac{M^2 m_{h\perp}^2}{Q^4}} \right) \,, \tag{A.5}$$

or in terms of η_h,

$$\zeta_h = \frac{\eta_h}{2} \left(1 + \sqrt{1 + 4\frac{1}{\eta_h^2} \frac{m_{h\perp}^2}{Q^2}} \right) \,. \tag{A.6}$$

One can show that for any finite ζ_h the variable $z_h \to \eta_h$ in the Bjorken limit. This is obviously true in any frame.

(p_h, q) frame. In this frame, used in ref. [17] for example, the external SIDIS vectors are defined as

$$p^\mu = p^+ \overline{n}^\mu + \frac{M_\perp^2}{2p^+} n^\mu + p_\perp^\mu \,, \tag{A.7a}$$

$$q^\mu = -\xi p^+ \overline{n}^\mu + \frac{Q^2}{2\xi p^+} n^\mu \,, \tag{A.7b}$$

$$p_h^\mu = \frac{m_h^2}{\zeta_h Q^2/\xi} p^+ \overline{n}^\mu + \zeta_h \frac{Q^2}{2\xi p^+} n^\mu \,, \tag{A.7c}$$

where $M_\perp^2 = M^2 - p_\perp^2 = M^2 + \boldsymbol{p}_\perp^2$ is the transverse mass of the target nucleon. The Nachtmann variable in this case is given by

$$\xi = \frac{2x_B}{1 + \sqrt{1 + 4x_B^2 M_\perp^2/Q^2}} \,, \tag{A.8}$$

which, in contrast to its definition in the (p, q) frame, depends explicitly on the transverse mass of the target nucleon. Furthermore, in terms of the fragmentation invariant z_h, the finite-Q^2 fragmentation variable ζ_h is given by

$$\zeta_h = \frac{z_h}{2} \frac{\xi}{x_B} \left(1 + \sqrt{1 - 4\frac{x_B^2}{z_h^2} \frac{M_\perp^2 m_h^2}{Q^4}} \right) , \tag{A.9}$$

or in terms of η_h by

$$\zeta_h = \frac{\eta_h}{2} \left(1 + \sqrt{1 + 4\frac{1}{\eta_h^2} \frac{m_h^2}{Q^2}} \right) . \tag{A.10}$$

$(\boldsymbol{p_h}, \boldsymbol{p})$ **frame.** The external vectors in this frame, used in ref. [18] for example, are given by

$$p^\mu = p^+ \overline{n}^\mu + \frac{M^2}{2p^+} n^\mu , \tag{A.11a}$$

$$q^\mu = -\xi p^+ \overline{n}^\mu + \frac{Q_\perp^2}{2\xi p^+} n^\mu + q_\perp^\mu , \tag{A.11b}$$

$$p_h^\mu = \frac{m_h^2}{\zeta_h Q^2/\xi} p^+ \overline{n}^\mu + \zeta_h \frac{Q^2}{2\xi p^+} n^\mu , \tag{A.11c}$$

where $Q_\perp^2 = Q^2 - q_\perp^2 = Q^2 + \boldsymbol{q}_\perp^2$ is the transverse mass of the virtual photon. The Nachtmann variable in this frame depends explicitly on $Q_\perp^2$,

$$\xi = \frac{Q_\perp^2}{Q^2} \frac{2x_B}{1 + \sqrt{1 + 4x_B^2 M^2 Q_\perp^2/Q^4}} , \tag{A.12}$$

and the finite-Q^2 fragmentation variable is given by

$$\zeta_h = \frac{z_h}{2} \frac{\xi}{x_B} \frac{Q^2}{Q_\perp^2} \left(1 + \sqrt{1 - 4\frac{x_B^2}{z_h^2} \frac{M^2 m_h^2}{Q^4}} \right) , \tag{A.13}$$

or

$$\zeta_h = \frac{\eta_h}{2} \frac{Q^2}{Q_\perp^2} \left(1 + \sqrt{1 + \frac{4}{\eta_h^2} \frac{m_h^2 Q_\perp^2}{Q^4}} \right) . \tag{A.14}$$

Relations between frames. In general the frames discussed here are distinct. However, to leading order in $1/Q^2$ the vectors p, q and p_h lie in the same plane and the three frames in fact coincide. Comparing the (p, q) and (p_h, q) frames, for example, the differences between the transverse momenta and scaling variables can be expressed as

$$\boldsymbol{p}_{h\perp} = \boldsymbol{p}_\perp^* + \mathcal{O}(\boldsymbol{p}_\perp^{*2}/Q^2) , \tag{A.15a}$$

$$\xi = \xi^* + \mathcal{O}(\boldsymbol{p}_\perp^{*2}/Q^2) , \tag{A.15b}$$

$$\zeta_h = \zeta_h^* + \mathcal{O}(\boldsymbol{p}_\perp^{*2}/Q^2) , \tag{A.15c}$$

where the asterisks (*) label quantities in the (p_h, q) frame. Similar relations are applicable also for the parton fractional momentum x and the hadron fractional momentum z. At leading order in collinear factorization one has $\boldsymbol{p}_{h\perp} = 0$ and the frames are manifestly equivalent. Moreover, since $\langle \boldsymbol{p}_{h\perp}^2 \rangle \ll Q^2$ for $\boldsymbol{p}_{h\perp}$-integrated cross sections at next-to-leading order the differences between the collinear frames should remain small. It will nevertheless be important to check whether, and in what kinematic range, this approximation is valid. On the other hand, for unintegrated cross sections the differences between frames become relevant and their effects must be quantified.

References

[1] I. Schienbein et al., *A review of target mass corrections*, *J. Phys.* **G 35** (2008) 053101 [arXiv:0709.1775] [SPIRES].

[2] O. Nachtmann, *Positivity constraints for anomalous dimensions*, *Nucl. Phys.* **B 63** (1973) 237 [SPIRES].

[3] H. Georgi and H.D. Politzer, *Freedom at moderate energies: masses in color dynamics*, *Phys. Rev.* **D 14** (1976) 1829 [SPIRES].

[4] K. Bitar, P.W. Johnson and W.-k. Tung, *QCD asymptotics and kinematic thresholds in deep inelastic scattering*, *Phys. Lett.* **B 83** (1979) 114 [SPIRES];
P.W. Johnson and W.K. Tung, *Structure functions and their moments as testing ground for QCD: the Pandora's box of mass effects*, Print-79-1018 (Illinois Tech) *Contribution to Neutrino '79*, Bergen, Norway, June 18-22, 1979.

[5] S. Matsuda and T. Uematsu, *Target mass effects in polarized electroproduction*, *Nucl. Phys.* **B 168** (1980) 181 [SPIRES].

[6] A. Piccione and G. Ridolfi, *Target mass effects in polarized deep-inelastic scattering*, *Nucl. Phys.* **B 513** (1998) 301 [hep-ph/9707478] [SPIRES].

[7] J. Blumlein and A. Tkabladze, *Target mass corrections for polarized structure functions and new sum rules*, *Nucl. Phys.* **B 553** (1999) 427 [hep-ph/9812478] [SPIRES].

[8] S. Kretzer and M.H. Reno, *Target mass corrections to electro-weak structure functions and perturbative neutrino cross sections*, *Phys. Rev.* **D 69** (2004) 034002 [hep-ph/0307023] [SPIRES].

[9] F.M. Steffens and W. Melnitchouk, *Target mass corrections revisited*, *Phys. Rev.* **C 73** (2006) 055202 [nucl-th/0603014] [SPIRES].

[10] R.K. Ellis, W. Furmanski and R. Petronzio, *Unraveling higher twists*, *Nucl. Phys.* **B 212** (1983) 29 [SPIRES].

[11] J.C. Collins, D.E. Soper and G. Sterman, *Factorization of hard processes in QCD*, *Adv. Ser. Direct. High Energy Phys.* **5** (1988) 1 [hep-ph/0409313] [SPIRES].

[12] J.C. Collins and D.E. Soper, *Parton distribution and decay functions*, *Nucl. Phys.* **B 194** (1982) 445 [SPIRES].

[13] S. Kretzer and M.H. Reno, *Tau neutrino deep inelastic charged current interactions*, *Phys. Rev.* **D 66** (2002) 113007 [hep-ph/0208187] [SPIRES].

[14] M.A.G. Aivazis, F.I. Olness and W.-K. Tung, *Leptoproduction of heavy quarks. 1. General formalism and kinematics of charged current and neutral current production processes*, *Phys. Rev.* **D 50** (1994) 3085 [hep-ph/9312318] [SPIRES].

[15] A. Accardi and J.-W. Qiu, *Collinear factorization for deep inelastic scattering structure functions at large Bjorken xB*, *JHEP* **07** (2008) 090 [arXiv:0805.1496] [SPIRES].

[16] A. Accardi and W. Melnitchouk, *Target mass corrections for spin-dependent structure functions in collinear factorization*, *Phys. Lett.* **B 670** (2008) 114 [arXiv:0808.2397] [SPIRES].

[17] S. Albino, B.A. Kniehl, G. Kramer and C. Sandoval, *Confronting fragmentation function universality with single hadron inclusive production at HERA and e^+e^- colliders*, *Phys. Rev.* **D 75** (2007) 034018 [hep-ph/0611029] [SPIRES].

[18] P.J. Mulders, *Transverse momentum dependence in structure functions in hard scattering processes*, lecture notes, http://www.nikhef.nl/~pietm/COR-0.pdf, unpublished (2001).

[19] O.W. Greenberg and D. Bhaumik, *Parton model with variable intermediate-state parton mass*, *Phys. Rev.* **D 4** (1971) 2048 [SPIRES].

[20] A. Bacchetta et al., *Semi-inclusive deep inelastic scattering at small transverse momentum*, *JHEP* **02** (2007) 093 [hep-ph/0611265] [SPIRES].

[21] J.C. Collins, T.C. Rogers and A.M. Stasto, *Fully unintegrated parton correlation functions and factorization in lowest order hard scattering*, *Phys. Rev.* **D 77** (2008) 085009 [arXiv:0708.2833] [SPIRES].

[22] J. Pumplin et al., *New generation of parton distributions with uncertainties from global QCD analysis*, *JHEP* **07** (2002) 012 [hep-ph/0201195] [SPIRES].

[23] B.A. Kniehl, G. Kramer and B. Potter, *Fragmentation functions for pions, kaons and protons at next-to-leading order*, *Nucl. Phys.* **B 582** (2000) 514 [hep-ph/0010289] [SPIRES].

[24] D. de Florian, R. Sassot and M. Stratmann, *Global analysis of fragmentation functions for pions and kaons and their uncertainties*, *Phys. Rev.* **D 75** (2007) 114010 [hep-ph/0703242] [SPIRES]; *Global analysis of fragmentation functions for protons and charged hadrons*, *Phys. Rev.* **D 76** (2007) 074033 [arXiv:0707.1506] [SPIRES].

[25] T. Navasardyan et al., *The onset of quark-hadron duality in pion electroproduction*, *Phys. Rev. Lett.* **98** (2007) 022001 [hep-ph/0608214] [SPIRES].

[26] HERMES collaboration, A. Airapetian et al., *Multiplicity of charged and neutral pions in deep-inelastic scattering of 27.5 GeV positrons on hydrogen*, *Eur. Phys. J.* **C 21** (2001) 599 [hep-ex/0104004] [SPIRES].

[27] EUROPEAN MUON collaboration, J. Ashman et al., *Forward produced hadrons in $\mu\, p$ and $\mu\, d$ scattering and investigation of the charge structure of the nucleon*, *Z. Phys.* **C 52** (1991) 361 [SPIRES].

[28] W. Melnitchouk, R. Ent and C. Keppel, *Quark-hadron duality in electron scattering*, *Phys. Rept.* **406** (2005) 127 [hep-ph/0501217] [SPIRES].

[29] F.E. Close and N. Isgur, *The origins of quark hadron duality: How does the square of the sum become the sum of the squares?*, *Phys. Lett.* **B 509** (2001) 81 [hep-ph/0102067] [SPIRES].

[30] F.E. Close and W. Melnitchouk, *Duality in semi-inclusive pion electroproduction*, *Phys. Rev.* **C 79** (2009) 055202 [arXiv:0902.4256] [SPIRES].

[31] H1 collaboration, C. Adloff et al., *Evolution of e p fragmentation and multiplicity distributions in the Breit frame*, *Nucl. Phys.* **B 504** (1997) 3 [hep-ex/9707005] [SPIRES].